Orientation relationships of phase transformation in α-$Al_{12}Mn_3Si$ pseudomorphs after plate-like Al_6Mn precipitate in an AA3004 Al-Mn based alloy

Hiroki Nakayasu[a,*], Equo Kobayashi[b], Tatsuo Sato[c], Randi Holmestad[d], Knut Marthinsen[e]

[a] Department of Metallurgy and Ceramics Science, Graduate School of Engineering, Tokyo Institute of Technology, 2-12-1 Ookayama, Meguro-ku, Tokyo 152-8550, Japan
[b] Department of Materials Science and Engineering, Tokyo Institute of Technology, Tokyo, Japan
[c] Tokyo Institute of Technology, Tokyo, Japan
[d] Department of Physics, Norwegian University of Science and Technology, Trondheim, Norway
[e] Department of Materials Science and Engineering, Norwegian University of Science and Technology, Trondheim, Norway

ABSTRACT

The phase transformation in the plate-like precipitates of Al_6Mn in an AA3004 Al-Mn based alloy, which was prepared by a chemical extraction technique, was investigated using transmission electron microscopy. The boiling-phenol method observed the entire range of possible shapes of the precipitates and the habit planes of the plate-like Al_6Mn were ⟨001⟩ in the sheet plane and ⟨110⟩ on its edges. The two orientation relationships between Al_6Mn and α-$Al_{12}Mn_3Si$ after the phase transformation is observed to be $[00\bar{1}]_6//[02\bar{3}]_\alpha$ and $(130)_6//(5\bar{3}2)_\alpha$ and $[00\bar{1}]_6//[1\bar{5}2]_\alpha$ and $(200)_6//(311)_\alpha$ (particles 1 and 2) (the suffixes 6 and α indicate zone axises or lattice planes of Al_6Mn and α-$Al_{12}Mn_3Si$ phases, respectively). The lattice misfits in these orientation relationships were observed to be −1.4% and 1.0%, respectively. Additionally, the thickness of the plate-like Al_6Mn was kept constant after transforming into the α-$Al_{12}Mn_3Si$ phase. Further, we did not observe any low index planes of the α-$Al_{12}Mn_3Si$ parallel to the (001) plane of the Al_6Mn, which means that the outlines of α-$Al_{12}Mn_3Si$ were constrained by the original shape of Al_6Mn, i.e., the transformed α-$Al_{12}Mn_3Si$ may be considered as a pseudomorph after Al_6Mn.

1. Introduction

Al-Mn based alloys are the most extensively used aluminum wrought alloys because of their good formability, high corrosion resistance, high galling resistance, and medium degree of strength. In this alloy series, the AA3004 alloy is applied to bodies of beverage cans. The general process to manufacture the sheets for these bodies includes casting, homogenization, hot and cold rolling, and annealing. During the homogenization process, supersaturated manganese precipitates as intermetallic dispersoids in the aluminum matrix. Metastable $Al_{12}Mn$ and stable Al_6Mn are the main dispersoids in the matrix in a high purity Al-Mn alloy system [1]. These intermetallic compounds precipitate in rhomboidal or rectangular plate-like shapes. However, common industrially used alloys contain silicon as one of the added or impurity elements. Consequently, in Al-Mn-Si alloy system, metastable Al_6Mn and stable α-$Al_{12}Mn_3Si$ form the main dispersoids [2]. Further, orthorhombic Al_6Mn precipitates in a plate-like shape [2] and the cubic α-$Al_{12}Mn_3Si$ precipitates in a granular shape [3] during heat treatments.

The primary Al_6Mn particles transform into α-$Al_{12}Mn_3Si$ by absorbing solute silicon atoms from the aluminum matrix [4–6], which is called the “6 to α transformation”. This transformation improves the galling resistance of the material [7] because the hardness of α-$Al_{12}Mn_3Si$ (HV ~900) [8] is higher than that of Al_6Mn (HV ~700) [8]. A similar transformation is also expected to occur in the Al_6Mn precipitates. However, it is difficult to directly observe this transformation using transmission electron microscopy (TEM), and very few observations have been reported for two reasons. Firstly, the shape of the precipitates, of which we can only observe the cross section of a plate-like precipitate (it looks like a bar [1]) in a thin TEM foil using a conventional sample preparation technique. In order to identify the orientation relationships of the phase transformation in the precipitates, the observation of the whole appearance of the plate-like precipitates is necessary, not only a cross sectional observation. The

Table 1
Chemical composition of the used AA3004 Al-Mn based alloy (mass%).

Sample	Mn	Mg	Fe	Si	Al
	0.99	1.01	0.26	0.15	Bal.

Table 2
Homogenization conditions in the present work.

Designation	Heating rate	Holding time	Cooling rate
S-R	50 K/h	16 h	W.Q.
R-R	Salt bath	16 h	W.Q.
S-S	50 K/h	16 h	50 K/h

second reason is their low number density. The observable area of a TEM sample prepared using conventional electropolishing begins usually some hundreds of nanometers from the edge of the holes. Thus, the probability that a plate-like precipitate will exist in this area is quite low. For these reasons, observing the orientation relationships in the "6 to α transformation" is difficult and has never been reported, as per our research.

In this study, a detailed investigation of the phase transformation in plate-like Al_6Mn to α-$Al_{12}Mn_3Si$ precipitates during homogenization treatment and annealing of an AA3004 alloy has been performed, using optical microscopy (OM), scanning electron microscopy (SEM), energy dispersive X-ray spectrometry (EDX), and TEM. The precipitates are chemically extracted from the matrix using the boiling-phenol method. Since the plate-like precipitates have a thickness equal to some dozens of nanometers, they can be directly observed in TEM by spreading them on a carbon film.

Table 3
Number density and average diameter of precipitates in the samples [19].

Sample	Number density of granular precipitates ($\times 10^3/m^2$)	Average diameter of granular precipitate (μm)	Number density of plate shaped precipitates ($\times 10^3/m^2$)
R-R	18.2	0.59	< 0.1
S-R	156	0.43	3.3
S-S	217	0.41	5.5

2. Experimental Procedure

The chemical composition of the DC cast AA3004 alloy investigated is shown in Table 1.

The homogenization treatment was conducted with a temperature accuracy of ± 5 K. Samples were heated to 853 K and held at this temperature for 16 h followed by cooling down to room temperature. The heating and cooling rates were varied to alter the size and dispersion of precipitates. Henceforth, samples are denoted according to the applied homogenization condition. For example, "S-R" means Slowly heated (50 K/h) and Rapidly cooled (water quench). The homogenization conditions are shown in Table 2. After homogenization, the samples were subsequently 90% cold rolled and annealed at 723 K for various times.

For optical microscopy, the samples were prepared by a standard metallographic procedure (grinding, polishing, and etching). 20 vol% sulfuric acid warmed to 353 K was selected as an etchant that makes it possible to determine the primary phases by color. For dispersoid extraction, we performed boiling-phenol method. Each sample was cut into pieces roughly 1 g each and placed in a flask containing 10 g phenol. Further, the flask was heated at 463 K in an oil bath. An Allihn condenser was attached to the top of the flask to reflux vaporized phenol. After partial dissolution of the matrix, some precipitates

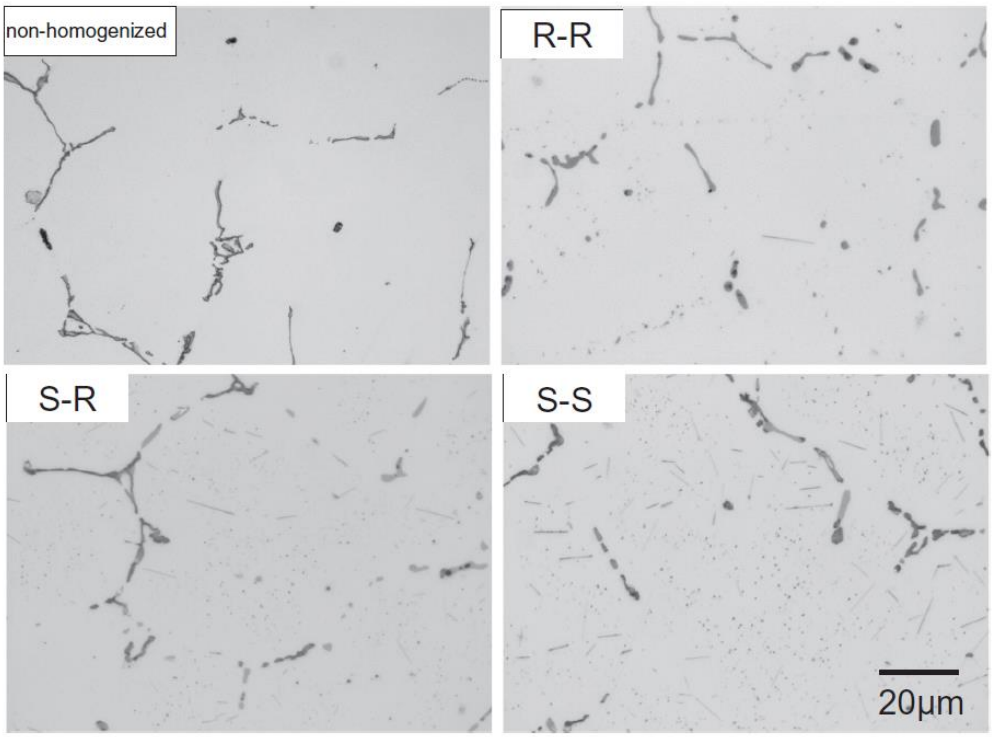

Fig. 1. Optical micrographs showing the microstructure of as-homogenized samples. (No-homo: as-cast sample, R-R: rapid heating and rapid cooling, S-R: slow heating and rapid cooling, S-S: slow heating and slow cooling) [19].

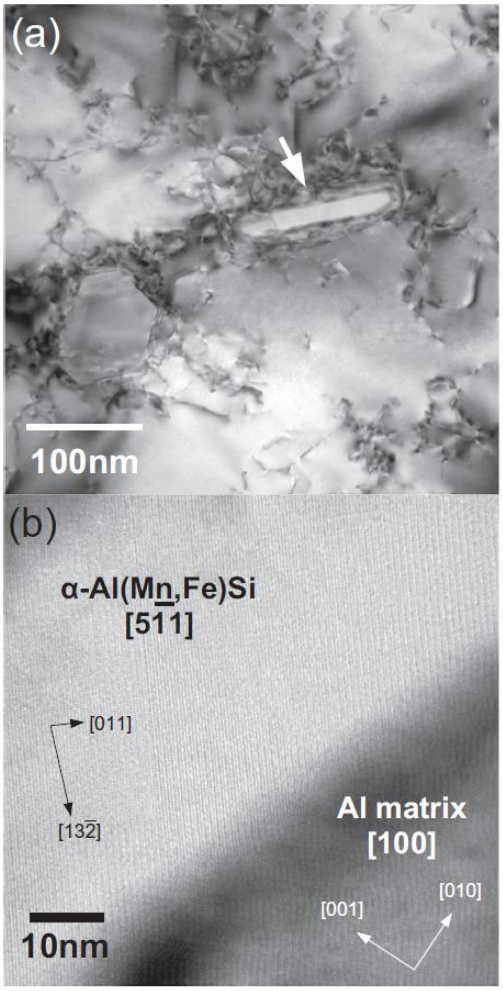

Fig. 2. TEM images of a plate-like precipitate in the S-S sample annealed at 723 K for 3 h after 90% cold rolling. (a) Bright field image and (b) high resolution image from the [100] zone axis in aluminum matrix.

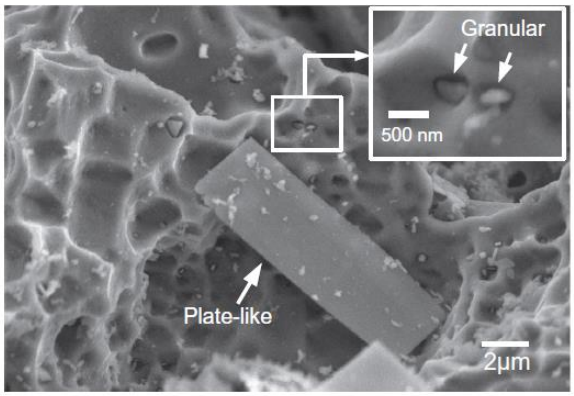

Fig. 3. SEM image showing typical plate-like and granular precipitate in the S-S as-homogenized sample.

remained on the dissolved surface which showing top half of their shape. SEM (15 kV, JSM-7000F, JEOL Co.) observations and EDX (JED-2300, JEOL Co.) analyses were conducted for this partially dissolved sample. For the matrix to be fully dissolved, 50 mL benzyl alcohol was added to the phenolic solution as a solidification inhibitor. The solution

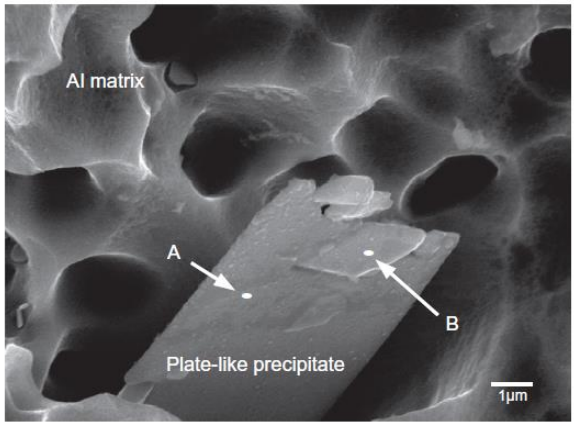

Fig. 4. SEM image exhibiting a plate-like precipitate extracted from the S-S as-homogenized sample.
EDX measurement points A and B presented in Table 4 are indicated in this image.

Table 4
EDX quantitative analysis results in points A and B in Fig. 4 (at.%).

Point	Al (σ)	Mn (σ)	Si (σ)	Mg (σ)
A	92.4 (0.1)	7.60 (0.8)	N. D.	N. D.
B	86.8 (0.1)	9.50 (0.7)	3.70 (0.1)	N. D.

N. D.: not detected.

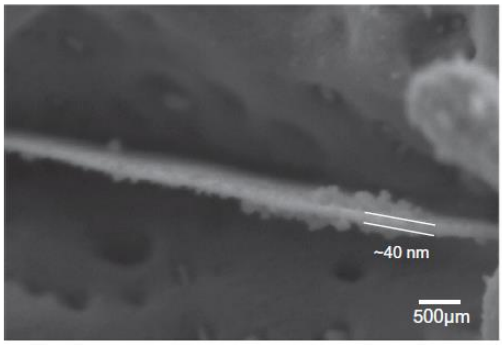

Fig. 5. SEM image of cross section of a plate-like precipitate in the S-S as-homogenized sample.

was further separated using suction filtration with a No. 2 filter paper. The residue was separated from the paper and suspended into acetone using an ultrasonic cleaner. The acetone containing extracted dispersoids were then dropped onto a molybdenum microgrid (RT-M10, STEM Co.) and naturally dried. TEM observations were conducted with a JEM-2100 (200 kV, double tilt holder, JEOL Co.) and a JEM-3010 (300 kV, double tilt holder, JEOL Co.). A lattice misfit ratio f was calculated according to the Eq. (1).

$$f = \frac{d_\alpha - d_6}{d_6} \times 100 \quad (1)$$

In Eq. (1), d_6 and d_α are the relevant lattice spacings mentioned in the orientation relationship of Al_6Mn and α-$Al_{12}Mn_3Si$, respectively. The relevant crystal structure models used for Al_6Mn and α-$Al_{12}Mn_3Si$ have been reported by Nicol [9] and Cooper et al. [10], respectively.

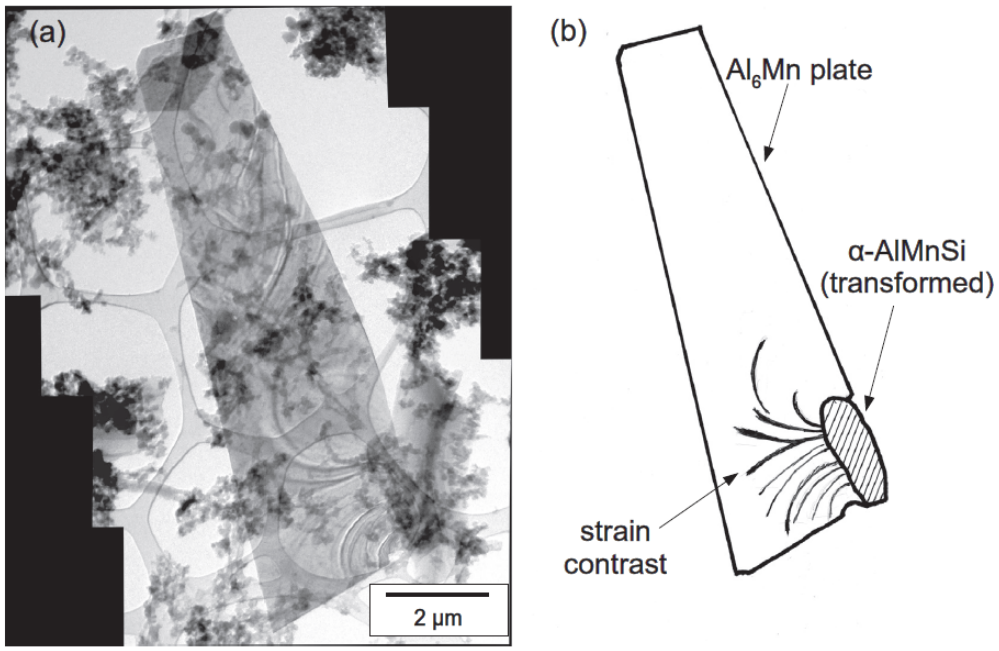

Fig. 6. (a) TEM bright field image and (b) schematic illustration showing a transformed region and strain contrast in a plate-like precipitate extracted from the S-S as-homogenized sample.

3. Results and Discussion

3.1. Plate-like Precipitates in Al Matrix

Optical micrographs of as-homogenized samples are shown in Fig. 1. In a non-homogenized sample, only black primary particles were observed. However, the phase transformation in primary particles and the precipitation occurred during homogenization treatments. Two types of precipitates were observed, i.e., granular and plate-like. Generally, it is known that α-AlMnSi exhibits a granular shape, whereas Al_6Mn exhibits a plate-like shape, respectively. In the R-R sample, the granular precipitates were coarser and sparser and the plate-like ones were clearly finer and fewer than those in the S-R sample, as expected. In the S-S sample, these were denser than those in the S-R sample, but their sizes were similar together with the number density of the plate-like precipitate. The number densities and average diameters of the granular precipitates from optical micrographs are shown in Table 3, which indicates average size in the S-S sample was very similar to that in S-R and that the number density was higher. These microstructures are in good agreement with those in a previous report [11].

A TEM bright field image of a plate-like precipitate in the S-S sample that was annealed at 723 K for 3 h is shown in Fig. 2(a). The sample was prepared using the conventional twin-jet method. The plate-like precipitate indicated by an arrow was identified as α-$Al_{12}Mn_3Si$ from the fast Fourier transformation (FFT) of the high resolution TEM (HR-TEM) image shown in Fig. 2(b). The sample was tilted to the [001] zone of the aluminum matrix. The sheet plane of the precipitate was identified as the (14-1) plane from the FFT image, which is not a low index plane.

From the plate-like shape shown (even though it is α-$Al_{12}Mn_3Si$), the hypothesis that this is a α-$Al_{12}Mn_3Si$ pseudomorph after the plate-like Al_6Mn precipitate can be derived. Pseudomorph is a phenomenon observed in mineralogy in which a compound is exhibiting an atypical shape from its crystal habit, resulting from constraints imposed by the original compound shape present before transformation or alternation. As per our knowledge, there are no studies mentioning pseudomorphs in metallic materials or intermetallic compounds. However, the plate-like α-$Al_{12}Mn_3Si$ was not euhedral because its faces were not low index planes, which is generally observed in a pseudomorph [12]. If this phenomenon occurs in the precipitate, it is presumably a transformation from Al_6Mn to α-$Al_{12}Mn_3Si$ which occurred during cooling and annealing, thus keeping the shape of the plate-like Al_6Mn precipitate.

3.2. Observation of Phase Transformation for Chemically Extracted Plate-like Precipitates

Chemical extraction of dispersoids was performed to prove the aforementioned hypothesis. The shape of precipitates was revealed by this technique. An SEM image of the S-S as-homogenized sample surface partially etched with the boiling phenol is shown in Fig. 3.

The typical plate-like and granular precipitates (white arrows in the enlarged insertion) in the matrix were clearly revealed using the etching technique. Fig. 4 shows a partially transformed plate-like precipitate in the same sample.

In the plate-like precipitate, there is a rhomboidal shaped region (indicated by point B) that has parallel planes and is slightly thicker than the plate in which it is embedded. EDX quantitative analysis results are shown in Table 4.

Only Al and Mn were detected at point A. Conversely, Si was detected together with Al and Mn at point B. In the Al-Mn-Si alloy system, various chemical formulae for the α-AlMnSi phase have been reported, i.e., $Al_{12}Mn_3Si$ [13–16], $Al_{15}Mn_3Si$ [17], and $Al_{10}Mn_2Si$ [4]. Watanabe et al. [8] reported that the α-AlMnSi phase that transformed from Al_6Mn primary particle in AA3004 was α-$Al_{12}Mn_3Si$. The Mn:Si ratio at point B was measured to be 2.6:1, which is close to the α-$Al_{12}Mn_3Si$. Consequently, it is reasonable to assume that the plate and the rhomboidal region are Al_6Mn and α-$Al_{12}Mn_3Si$, respectively. A higher Al content than the stoichiometric composition of both intermetallic compounds is considered to be a result of the transmission of the electron beam and thus mixing of characteristic X-ray signals, which further reflects the effects of the Al matrix beneath the precipitates. Fig. 5 shows a SEM image of the cross section of a plate-like precipitate. Its thickness was approximately 40 nm, which is sufficiently thin for direct TEM observations.

A TEM BF image of an Al_6Mn plate-like precipitate extracted from

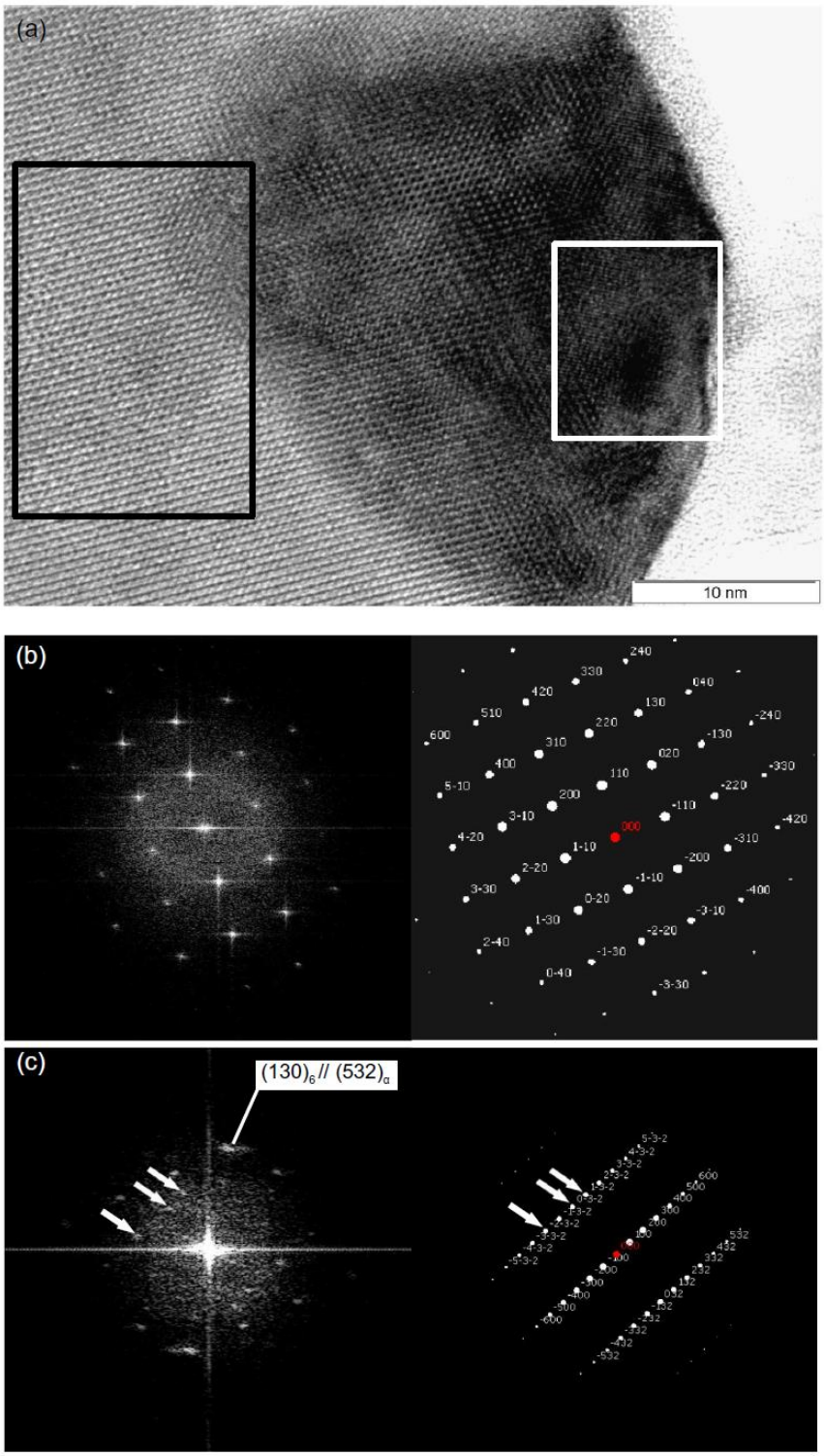

Fig. 7. (a) HR-TEM image of partially transformed plate-like precipitate extracted from S-S as-homogenized sample. (b) FFT image of black rectangle area in (a) and a simulated diffraction pattern of Al6Mn from [00$\bar{1}$] zone axis. (c) FFT image of white rectangle area in (a) and a simulated diffraction pattern of α-Al12Mn3Si from [02$\bar{3}$] zone axis. The remarked α-Al12Mn3Si spots are indicated by white arrows both on the FFT image and the simulated diffraction pattern.

the S-S as-homogenized sample is shown together with a schematic illustration of the same configuration in Fig. 6.

Its right bottom corner is the area that was transformed to α-$Al_{12}Mn_3Si$. Further, strain contrast due to the lattice misfits between Al_6Mn and α-$Al_{12}Mn_3Si$ is observed around the transformed area. An HR-TEM image of a partially transformed plate-like precipitate in S-S as-homogenized sample (note: this is a different precipitate than that shown in Fig. 6) is shown in Fig. 7(a). The sample was tilted to the [00$\bar{1}$] zone axis of Al_6Mn. The FFT images of the regions in Fig. 7(a) are shown in Fig. 7(b) showing that the habit planes were ⟨001⟩ in its sheet plane and ⟨110⟩ on its edges. From Fig. 7(b) and (c), the transformation relationships can be written as

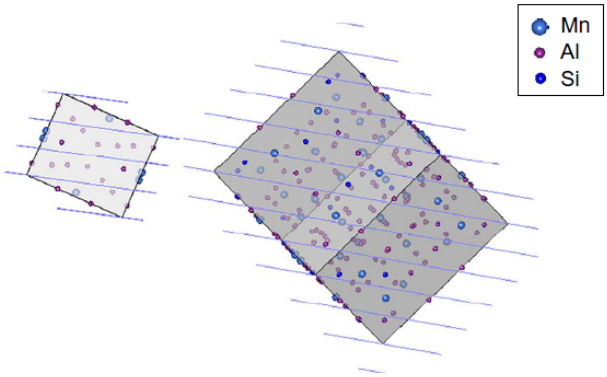

Fig. 8. A schematic illustration showing an orientation relationship of the "6 to α transformation" from Al_6Mn to α-$Al_{12}Mn_3Si$. The orientation relationship can be written as $[00\bar{1}]_6//[02\bar{3}]_\alpha$ and $(130)_6//(\bar{5}32)_\alpha$. Blue lines indicate parallel planes in this relationship. (For interpretation of the references to color in this figure legend, the reader is referred to the web version of this article.)

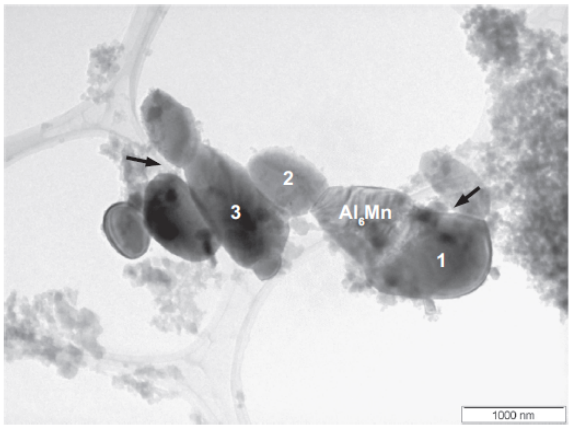

Fig. 9. TEM bright field image showing a group of granular precipitates. Gaps between particles are indicated by black arrows.

$[00\bar{1}]_6//[02\bar{3}]_\alpha$ and $(130)_6//(5\bar{3}2)_\alpha$

Hereafter, the suffixes 6 and α indicate zone axes or lattice planes of Al_6Mn and α-$Al_{12}Mn_3Si$ phases, respectively. In Fig. 7(c) not only α-$Al_{12}Mn_3Si$ spots, but also Al_6Mn spots are seen (α-$Al_{12}Mn_3Si$ spots are indicated by white arrows). The lattice misfit in this case is − 1.4%, and a schematic illustration of the current orientation relationship is shown in Fig. 8. It can be assumed that the transformation in this orientation relationship is easy because of the small misfit.

Fig. 9 shows a group of granular particles extracted from the S-S sample annealed at 723 K for 3 h. These particles are connected to the Al6Mn plate. Some gaps between the particles can be observed in Fig. 9. The particle group was observed only in annealed samples, not in as-homogenized samples.

Fig. 10 shows a schematic illustration indicating a possible mechanism for the particle group formation. Alexander et al. [7] reported that the "6 to α transformation" produces aluminum spots by the eutectoid reaction, which is described in formula (2).

$$3Al_6Mn + Si \rightarrow \alpha\text{-}Al_{12}Mn_3Si + 6Al \quad (2)$$

When the phase transformation occurs in the Al_6Mn plate, some Al is produced in the vicinity of the α-$Al_{12}Mn_3Si$ particles. The produced Al is dissolved by the boiling phenol during the chemical extraction step. Thus, some Al_6Mn plate pieces and α-$Al_{12}Mn_3Si$ particles are separated and some particles connected with Al_6Mn and α-$Al_{12}Mn_3Si$ are left as a particle group. Fig. 11 shows the diffraction patterns of the particles 1 to 3 and Al_6Mn which is shown in Fig. 9.

Particles 1 and 2 shown in Fig. 9 had the same orientation and disk shape, which could mean that the Al_6Mn plate was transformed to α-$Al_{12}Mn_3Si$ while keeping its sheet plane. From the diffraction patterns of Al_6Mn and particles 1 and 2 in Fig. 9, the orientation relationships of the "6 to α transformation" in this group can be written as

$[00\bar{1}]_6//[1\bar{5}2]_\alpha$ and $(200)_6//(311)_\alpha$ (particles 1 and 2)

A schematic illustration of the present orientation relationship is illustrated in Fig. 12.

In this orientation relationship, the lattice misfit is 1.04%, i.e., this orientation relationship also has a small misfit. If a slice of a particle group was observed in a TEM sample prepared using the conventional twin-jet method, it would look similar to the precipitates in Fig. 2(a). It is noted that only a little area of the plate-like precipitate was transformed into the α-Al12Mn3Si phase in this figure. Particle 3, which was shown in Fig. 9, was identified as $[\bar{1}2\bar{9}]$ direction of Al6Mn. This direction has 10 degrees tilt from $[00\bar{1}]$ zone axis, which is caused by the sample bending.

All the observed orientation relationships have lattice misfits smaller than 1.5%. Consequently, the "6 to α transformation" easily occurs in these cases as it is giving orientation relationships that all have small lattice misfits.

From the orientation relationships found, not all of the surfaces of

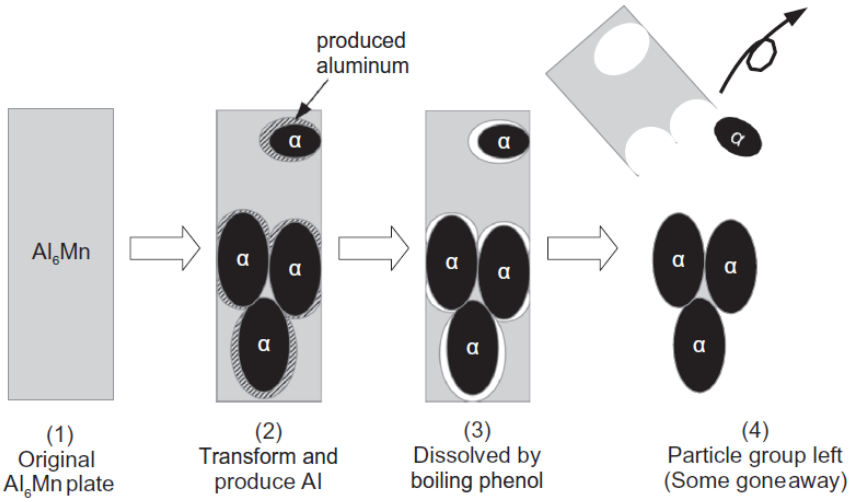

Fig. 10. Schematic illustration showing a process of forming a particle group; (1) original Al_6Mn plate, (2) phase transformation occurred and Al was produced between Al_6Mn and α-$Al_{12}Mn_3Si$, (3) dissolution of produced Al was dissolved by boiling phenol, (4) some particles connected with intermetallic compounds were maintained as a group of particles.

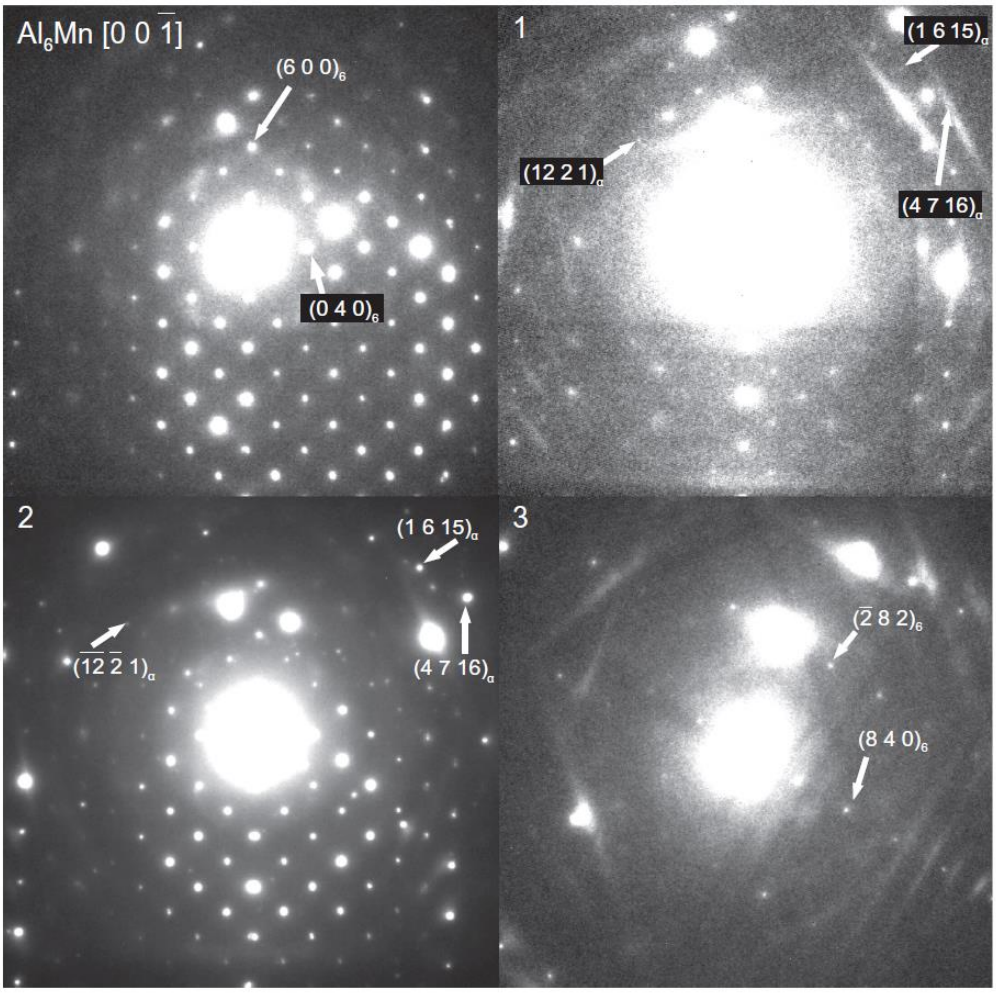

Fig. 11. Diffraction patterns from each of the particles designated in Fig. 9.

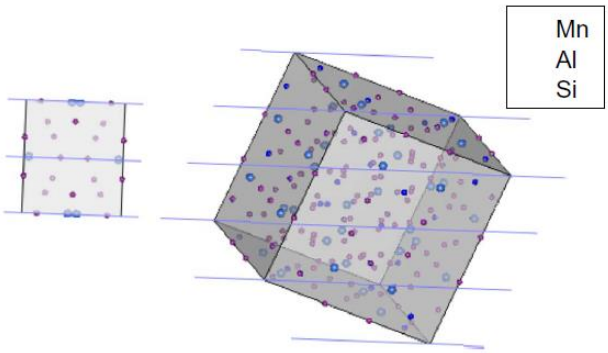

Fig. 12. A schematic illustration showing an orientation relationship of the "6 to α transformation" from Al_6Mn to α-$Al_{12}Mn_3Si$. The orientation relationship can be written as $[00\bar{1}]_6//[1\bar{5}2]_\alpha$ and $(200)_6//(311)_\alpha$. Blue lines indicate parallel planes in this relationship. (For interpretation of the references to color in this figure legend, the reader is referred to the web version of this article.)

the transformed α-$Al_{12}Mn_3Si$ regions parallel to the original Al_6Mn plates were low index planes. If the shape of the α-$Al_{12}Mn_3Si$ particles was euhedral, the surfaces should all have low Miller indices according to the law of simple rational indices [18]. This phenomenon often occurs in pseudomorphs. When the shape of the transformed compound, in this case α-$Al_{12}Mn_3Si$, is constrained by the shape of the original compound, in this case Al_6Mn, the plane that becomes the surface is determined by the orientation relationship of the phase transformation. Because of this constraint, the surface of the transformed region is generally not a euhedral plane, but a high Miller index plane.

4. Conclusion

It is demonstrated that the boiling phenol method is a useful technique to observe precipitates in aluminum alloys using SEM and TEM. The plate-like Al_6Mn extracted by this method was sufficiently thin in thickness to conduct HR-TEM observations (~40 nm) and made it possible to directly observe the phase transformation in plate-like precipitates. The EDX analysis showed that only the transformed regions of the plate-like Al_6Mn precipitates contained Si, and the Mn:Si ratio was observed to be 2.6:1. Therefore, the transformed region in Al_6Mn plate-like precipitates was identified as the α-$Al_{12}Mn_3Si$ phase. The habit planes of the Al_6Mn plate-like precipitate were < 001 > in the sheet plane and < 110 > on its edges. As a result, the observed orientation relationships between Al_6Mn and α-$Al_{12}Mn_3Si$ in an Al_6Mn plate-like precipitates can be written as

$[00\bar{1}]_6//[02\bar{3}]_\alpha$ and $(130)_6//(\bar{5}32)_\alpha$

$[00\bar{1}]_6//[1\bar{5}2]_\alpha$ and $(200)_6//(311)_\alpha$

Furthermore, the corresponding lattice misfits of these orientation relationships were − 1.4% and 1.04%, respectively. Further, both the observed orientation relationships of the “6 to α transformation” thus had lattice misfits lower than 1.5%, which make it easy to transform with these orientation relationships. The “6 to α transformation” proceeded by absorbing solute Si atoms while keeping the thickness and shape of the plate-like Al_6Mn, which is called a pseudomorph in mineralogy. The plate-like α-$Al_{12}Mn_3Si$ observed in the annealed samples are considered to be formed as pseudomorphs because the flat surfaces parallel to original plates were not low index planes.

References

[1] P. Yang, O. Engler, H.J. Klaar, J. Appl. Crystallogr. 32 (1999) 1105–1118.
[2] Y.J. Li, W.Z. Zhang, K. Marthinsen, Acta Mater. 60 (2012) 5963–5974.
[3] Y.J. Li, Lars Arnberg, Light Metals, 2003 (2003), pp. 991–997.
[4] H. Hanemann, A. Schrader, Teraere Legierungun des Aluminiums, Velag Stahleisen M. B. H., 1952.
[5] Y.J. Li, L. Arnberg, Mater. Sci. Eng. A 347 (2003) 130–135.
[6] Y.J. Li, A. Johansen, S. Benum, C.J. Simensen, A.L. Dons, A. Hakonsen, Aluminium 80 (2004) 578–583.
[7] D.T.L. Alexander, A.L. Greer, Acta Mater. 50 (2002) 2571–2583.
[8] H. Watanabe, K. Ohori, Y. Takeuchi, Jpn. Inst. Light Met. 33 (1982) 149–156.
[9] A.D.I. Nicol, Acta Cryst 6 (1953) 285–293.
[10] M. Cooper, K. Robinson, Acta Cryst 20 (1966) 614–617.
[11] Y.C. Lee, E. Kobayashi, T. Sato, Korean J. Mater. Res. 24 (2014) 229–235.
[12] J. Theo Kloprogge, Rob Lavinsky, Stretch Young: Photo Atlas of Mineral Pseudomorphism, Elsevier, 2017, p. 18.
[13] H. Warlimont, Aluminium 53 (1977) 171.
[14] G. Hausch, P. Furrer, H. Warlirriont, Z. MetalIkd. 69 (1978) 174.
[15] P. Furrer, G. Hausch, Met. Sci. 13 (1979) 155.
[16] P. Furrer, Z. Metallkd. 70 (1979) 699.
[17] L. Bäckerud, E. Król, J. Tamminen, Solidification Characteristics of Aluminum Alloys, 1 Universitetsforlaget, Oslo, 1986.
[18] T. Nagase, J. Crystallogr. Soc. Jpn. 40 (2000) 469–473.
[19] H. Nakayasu, E. Kobayashi, T. Sato, Jpn. Inst. Light Met. 67 (2017) 438–444.